Biocontrol Potential of *Bacillus velezensis* against *Sclerotium rolfsii* Causing Stem Rot in *Arachis hypogaea* L.

Madison Claire Reynolds [1*], Benjamin Scott Harrison [2]

[1] USDA Agricultural Research Service, National Peanut Research Laboratory, Dawson, USA
[2] Department of Plant Pathology, North Carolina State University, Raleigh, USA

*Corresponding author: **Madison Claire Reynolds**

Received: 13 Dec 2024
Revised: 31 Dec 2024
Accepted: 12 Jan 2025
Published: 04 Feb 2025

E-ISSN: 2989-5340
DOI: https://doi.org/10.54660/jafi.2025.5.1.55-66

ABSTRACT

Background: *Sclerotium rolfsii* Sacc. causes stem rot. is a serious soil-borne constraint to groundnut (*Arachis hypogaea* L.) production and can cause yield losses ranging from 25 to 80% under conducive conditions. Chemical fungicides have limited residual activity and are of concern from an environmental sustainability perspective so biologically based management alternatives are needed.

Objectives: To assess the biocontrol potential of *Bacillus velezensis* strain BV-TNAU17 against S. rolfsii under *in vitro* and pot and field conditions. To determine the antagonistic mechanisms such as lipopeptide production, hydrolytic enzyme activity and induced systemic resistance. To evaluate the plant growth promoting properties under pathogen stress.

Materials and Methods: To evaluate the biocontrol potential of *Bacillus velezensis* strain BV-TNAU17 against S. rolfsii under *in vitro* and pot and field conditions. To study the antagonistic mechanisms such as lipopeptide production, hydrolytic enzyme activity and induced systemic resistance. For determination of the plant growth promoting properties under pathogen stress.

Results: BV-TNAU17 inhibited the growth of S. rolfsii mycelium by 72.4% in dual culture and produced iturin A, fengycin and surfactin lipopeptides as identified by HPLC-MS analysis. Under field conditions, seed treatment with BV-TNAU17 plus soil drench reduced the disease incidence by 68.3%, disease severity by 71.6% and increased the pod yield by 44.2% over pathogen inoculated control. BV-TNAU17 treated plants showed significant increase in activities of defense enzymes (peroxidase, polyphenol oxidase and phenylalanine ammonia-lyase) suggesting induced systemic resistance. Rhizosphere microbial biomass carbon increased by 38.7% and urease activity by 31.4% relative to untreated inoculated controls.

Conclusion: B. velezensis BV-TNAU17 exhibited multi-faceted biocontrol mechanisms and plant growth-promotion properties, which altogether suppress S. rolfsii and enhance the groundnut productivity. This strain has a promising prospect to be a part of integrated disease management strategies for sustainable groundnut cultivation.

Keywords: biocontrol; *Bacillus velezensis*; *Sclerotium rolfsii*; groundnut; stem rot; lipopeptides; induced systemic resistance; plant growth promotion; integrated disease management; soil-borne pathogen

1. Introduction

1.1. Importance of Groundnut

Groundnut (*Arachis hypogaea* L.) is one of the most important legumes and oil seeds in the world. Groundnut is cultivated throughout the tropical and subtropical climatic zones in Asia, Africa and the Americas (FAO, 2023) [1]. Globally, the area under groundnut cultivation is about 31.5 million hectares, with an estimated annual production of around 49 million metric tonnes. India is the second largest groundnut producer in the world after China, accounting for about 22% of the total world groundnut production, and it is a rich source of proteins (25–30%) and edible oil (44–55%) as well as several micronutrients, providing sustenance to the millions of small farmers (Directorate of Groundnut Research, 2023) [2]. Groundnut is also an important fodder crop in crop-livestock production systems. It has agricultural significance because of its nitrogen-fixing properties and is widely used for the preparation of cakes and meals after oil extraction (Vessey, 2003) [20].

The economic significance of groundnut can be seen in a number of different sectors. Confectionery and peanut butter production, as well as medicine, all require that farmers have a reliable supply of the right types of nuts. Even though the groundnut does a good job at fixing nitrogen and has good agricultural adaptations, its productivity in terms of production per hectare is still low in spite of the seeds' potential to produce large quantities of nuts. It has been found that the average pod yield in India is around 1.2-1.5 tons per hectare, while the potential is believed to be about 4-5 tons per hectare (Directorate of Groundnut Research, 2023) [2]. The difference in yields has been attributed to both abiotic and biotic factors affecting the crop including environmental factors such as drought and heat and pests. Out of all the problems posed by biotic factors, the ones associated with diseases caused by soil fungi are especially serious (Punja, 1985) [4] (Aycock, 1966) [3].

1.2. Stem Rot Disease

Stem rot of groundnut, also called white mold or southern blight in different regions, is caused by the hemibiotrophic, multi-host soilborne pathogen *Sclerotium rolfsii* Sacc. [teleomorph: *Athelia rolfsii* (Curzi) Tu & Kimbrough] (Aycock, 1966) [3] (Punja, 1985) [4]. It can be found in all agro-climatic zones of groundnut cultivation but is prevalent in warm, humid conditions with a soil temperature of 25-30 Degrees Celsius and ample rainfall or irrigation water (Punja, 1985) [4] (Cilliers *et al*., 1993) [6]. The disease can result in yield loss of 25-80% in cases of epidemics and complete crop failure in very infested fields during the conducive periods (Punja, 1985) [4] (Cilliers *et al*., 1993) [6].

The main infection process consists in the formation of fans-like mycelial mats at the base of the stem, hypocotyl, and within the root collar of the young and mature plants. Infected tissues become water-soaked, brown, and even collapse causing characteristic wilting and death of the whole plant. The application of adequate amount of white fluffy fungal mycelium and black structures known as sclerotia of about the size of mustard seeds, appearing on the soil surface and infected plant parts, makes diagnosis easy. Sclerotia are formed structures that consist of dark fruiting body which is densely packed with the fungus and survives in the ground for 2-5 years absence of susceptible host plant (Aycock, 1966) [3]. Control of stem rot is complicated due to the lack of resistant crop varieties release and thus reliance on fungicides and other cultural practices (Punja, 1985) [4].

The repeated use of fungicides creates favorable conditions for fungi to develop resistance, pollutes soil and water sources, kills useful microorganisms in soil, and threatens human health due to the build-up of residues in food (Köhl *et al*., 2019) [12]. Such disadvantages have led to growing scientific and policy interest in biological pest management techniques for groundnut stem root disease due to their sustainable and residue-free nature (Köhl *et al*., 2019) [12] (Shoda, 2000) [17].

1.3. Biology of *Sclerotium rolfsii*

Based on molecular phylogenetic studies that place its teleomorph *Athelia rolfsii* to the phylum *Basidiomycota*, *Sclerotium rolfsii* (Sacc.) belongs to the *Cantharellales* order and *Polyporaceae* family (Okabe and Matsumoto, 2000) [5]. The fungus is characterized by the formation of white, superficial aerial mycelium appearing from the center of infection in form of fan-shaped armillaries. The hyphae consist of thin-walled branched structures with a diameter of about 5–8 µm, clamped at the septa. Sclerotia appear in white to tan and can grow to be 0.5-3.0 mm in diameter. The smooth and solid texture of the sclerotia contributes to their resistance to UV, desiccation, strenuous soil treatments, and some of the chemical compounds used as fungicides that could otherwise destroy them (Okabe and Matsumoto, 2000) [5] (Cilliers *et al*., 1993) [6].

Pathogenicity of S. rolfsii relies heavily on a complex set of cell wall degrading enzymes (CWDEs) and toxic organic compounds. Oxalic acid, which is released in millimolar concentrations in advance of the growing mycelium, is responsible for calcium chelation from host cell walls; it can also decrease the soil pH to around 2 to 4 and cause direct death of the plant tissue. Polygalacturonase, Pectin methylesterase, cellulose, and xylanase attack plant tissue and make it easier for S. rolfsii to colonize complicated plant body (Cilliers *et al*., 1993) [6]. In addition, the fungus produces a number of non-enzymatic effector proteins that inhibit ROS bursts in host cells and suppress defensive reaction of the host plant. Thus, a combination of enzymatic action, acidic molecular disruption, and inhibition of host plant immunity gives the pathogen considerable advantage and makes it possible to kill the plant cells simply by coming into contact with them in appropriate weather conditions (Punja, 1985) [4].

The cycle of S. rolfsii infection begins when sclerotia germinate due to root exudates, volatile organic compounds, and increased soil moisture after rainfall or irrigation. Sclerotia produce infections cushions and hyphae that penetrate the outer layer of cells through direct contact or natural openings. The growth of mycelia is responsible for the expansion of lesions as well as the formation of new sclerotia on the periphery of colonies that will be dispersed through moves in the soil's waters and tillage equipment. S. rolfsii will spread inside the fields and create dead patches along crop rows. The disease's severity increases as the season advances until it reaches its highest point during flowering and pod-filling periods. The sexual phase of S. rolfsii (*Athelia rolfsii*) can deal in the sexual reproductive phase, but its ecology is less Important in the life cycle of S. rolfsii than the ecology of its asexual reproductive phase (sclerotia). The complete cycle is illustrated in Fig. 1 (see Section 4) (Aycock, 1966) [3] (Punja, 1985) [4].

2. Biology of *Bacillus velezensis*

Bacillus velezensis Ruiz-García *et al*. (2005) is a Gram-positive, spore-forming, rod-shaped bacterium belonging to the *Bacillus subtilis* group of organisms within the phylum Firmicutes (Ruiz-García *et al*., 2005) [7]. It was first isolated from soil samples obtained from the locality of Vélez-Málaga, Spain, and describes a new species in terms of its phenotypic and chemotaxonomical features. Recently molecular techniques including multi-locus sequence typing, comparative genomics, and average nucleotide identity analysis have confirmed that B. velezensis is different from the related species B. subtilis, B. amyloliquefaciens, and B. siamensis, resulting in the restructuring of the bacterial classification system (Chowdhury *et al*., 2015) [8]. It has been found that this species comprises many strains that were once classified under the name of *Bacillus amyloliquefaciens* subsp. *plantarum* (Ruiz-García *et al*., 2005) [7].

The genome of B. velezensis usually has an average of 3.9 to 4.2 Mb with more than 12 to 14 biosynthetic group of genes (BGCs) responsible for the synthesis of secondary metabolites with antagonistic abilities towards phytopathogenic fungi and bacteria. These BGCs produce the biological parts necessary for synthesis of lipopeptides, polyketides, and siderophores (Ruiz-García *et al*., 2005) [7]. The fragment of the genome characteristic of the biosynthesis of the secondary metabolites in the case of B. velezensis is about 8.5 to 9.0%, which is among the highest ones among plant-associated and beneficial bacterial genomes (Chowdhury *et al*., 2015) [8]. This emphasis of the genome on the matter of the secondary metabolites' synthesis gives B. velezensis a layered approach to biocontrol which cannot be easily overcome by any evolutionary counter-attack of the pathogen.

2.1. Antagonistic Mechanisms

The antagonistic activity of B. velezensis against soil-borne and aerial phytopathogens operates through a hierarchical set of mechanisms that collectively suppress pathogen establishment, growth, and pathogenicity. These mechanisms can be broadly categorized as direct suppression—comprising lipopeptide-mediated membrane disruption, antibiotic production, and hydrolytic enzyme secretion—and indirect suppression through competitive exclusion, induced systemic resistance, and phytohormone-mediated growth promotion (Ruiz-García *et al*., 2005) [7] (Shan *et al*., 2022) [9]. The relative contribution of each

mechanism varies with soil type, inoculum density, plant developmental stage, and environmental conditions, explaining why B. velezensis-based biocontrol products often outperform single-mode agents under diverse field conditions (Shan *et al*., 2022) [9].

2.2. Rhizosphere Colonization

Effective biocontrol by B. velezensis is contingent on its ability to colonize the root surface and rhizosphere zone persistently over the crop growth cycle. Root colonization is mediated by chemotaxis toward root exudate components—particularly malic acid, fumaric acid, sugars, and amino acids—that activate CheA/CheY two-component signaling systems to direct bacterial swimming toward roots (Shan *et al*., 2022) [9]. Upon root contact, flagellar rotation enables surface scanning, followed by EpsE-mediated flagellum immobilization and transition to surface-associated motility via SrfA surfactin-mediated spreading. Anchoring of bacterial cells to root epidermis involves polysaccharide adhesins (EPS, levan, poly-γ-glutamate), TasA protein fibers of the biofilm matrix, and hydrophobic surface layer proteins. Established microcolonies expand into three-dimensional biofilms that ensheath the root surface in a protective bacterial carpet, physically excluding competing pathogens and delivering bioactive compounds at concentrations sufficient to suppress pathogen germination and growth within the root's immediate microenvironment (Shan *et al*., 2022) [9] (Chen *et al*., 2018) [10].

2.3. Lipopeptides

Lipopeptides constitute the primary direct antifungal effectors produced by B. velezensis. Iturin A is a cyclic heptapeptide linked to a C_{14}–C_{17} β-amino fatty acid chain, synthesized non-ribosomally by the ItuA-D multienzyme complex. Iturin A inserts into fungal plasma membranes and forms ion channels that dissipate membrane potential, cause uncontrolled ion flux, and rupture lipid bilayers, leading to fungal cell lysis (Chen *et al*., 2018) [10]. Scanning electron microscopy of S. rolfsii hyphae exposed to iturin A fractions from B. velezensis reveals extensive plasma membrane blistering, cytoplasmic leakage, and hyphal collapse within 6–12 hours of exposure. Fengycin (plipastatin), a lipodecapeptide with a C_{14}–C_{18} fatty acid tail, targets membrane-bound phospholipases and inhibits spore germination and germ-tube elongation. Surfactin, a cyclic lipoheptapeptide biosurfactant, contributes to biocontrol through membrane permeabilization at higher concentrations, competitive surface colonization at lower concentrations, and elicitation of plant defense signaling through its structural similarity to lipopolysaccharide-derived elicitors (Chen *et al*., 2018) [10] (Ding *et al*., 2005) [11].

2.4. Hydrolytic Enzymes

Beyond lipopeptides, B. velezensis secretes a spectrum of extracellular hydrolytic enzymes that degrade fungal cell wall components and compromise pathogen structural integrity. Chitinase degrades chitin, a principal structural polysaccharide of fungal cell walls, releasing chitooligomers that simultaneously attenuate fungal viability and function as damage-associated molecular patterns (DAMPs) that prime plant immune responses. β-1,3-glucanase hydrolyzes callose and laminarin-type glucans in fungal cell walls, synergizing with chitinase to cause irreversible cell wall damage. Protease activity degrades fungal cell wall proteins and germination-stimulating lectins. Cellulase and amylase activities contribute to substrate competition in the rhizosphere, where carbon availability is a primary determinant of microbial competitive fitness (Ding *et al*., 2005) [11]. The combined activity of these enzymes produces a mycoparasitic-like suppressive microenvironment at the root surface that significantly reduces sclerotial germination rates and inhibits penetration hyphae formation by S. rolfsii (Köhl *et al*., 2019) [12].

2.5. Biofilm Formation

Biofilm formation represents a critical ecological strategy by which B. velezensis achieves persistent root colonization and sustained delivery of bioactive compounds. Biofilm development proceeds through four distinct stages: initial surface attachment (motility-dependent), microcolony formation (matrix synthesis-dependent), biofilm maturation (involving channels and water retention), and dispersal (triggered by nutrient depletion and quorum-sensing signals). The biofilm extracellular matrix comprises TasA protein fibers, exopolysaccharides, poly-γ-glutamate, and surfactin biosurfactant, collectively creating a structured, desiccation-resistant community architecture (Köhl *et al*., 2019) [12]. Quorum-sensing signals—N-acyl homoserine lactones and cyclic lipopeptides in particular—coordinate biofilm gene expression across the community, ensuring that antifungal gene clusters are upregulated precisely when pathogen-derived volatile cues are detected. Biofilm-encased bacteria on roots exhibit 10–100-fold greater tolerance to soil fungicides, UV radiation, desiccation, and predation by soil fauna compared to planktonic cells, explaining the superior field persistence of biofilm-competent strains relative to non-biofilm-forming mutants (Köhl *et al*., 2019) [12] (Niu *et al*., 2011) [13].

2.6. Induced Systemic Resistance

Induced systemic resistance (ISR) conferred by B. velezensis represents a physiologically primed state of heightened defensive capacity in the host plant, activated without prior pathogen challenge. ISR-triggering determinants include lipopolysaccharides (LPS), flagellins, exopolysaccharides, volatiles (2,3-butanediol, acetoin), siderophores, and lipopeptides produced by the rhizobacterium (Niu *et al*., 2011) [13]. These microbe-associated molecular patterns (MAMPs) are perceived by pattern recognition receptors (PRRs)—including FLS2 (flagellin-sensitive 2) and EFR (EF-Tu receptor)—on root epidermal cells, activating MAPK cascades and downstream transcription factor networks (WRKY, MYC2) that upregulate jasmonic acid (JA) and ethylene (ET) biosynthesis while leaving salicylic acid (SA) levels unchanged. This JA/ET-dependent ISR is phenotypically expressed in distal, uninoculated leaves and stems as a 'primed' state, characterized by faster and stronger activation of defense gene transcription following pathogen challenge, reduced lesion size, and systemic accumulation of defense-related enzymes including peroxidase (POX), polyphenol oxidase (PPO), phenylalanine ammonia-lyase (PAL), and pathogenesis-related (PR) proteins (Niu *et al*., 2011) [13] (Backer *et al*., 2018) [14]. The ISR phenotype in groundnut treated with B. velezensis has been demonstrated to persist for 40–50 days after seed treatment, well beyond the period of maximum stem rot susceptibility at the seedling stage, providing a critical window of protection during the most vulnerable phases of crop establishment (Backer *et al*., 2018) [14].

2.7. Plant Growth Promotion

Beyond pathogen suppression, B. velezensis directly promotes plant growth through multiple mechanisms that increase nutrient availability, modulate phytohormone balance, and improve root architecture. Phosphate solubilization, mediated by gluconic acid secretion and phosphatase activity, releases plant-available

orthophosphate from sparingly soluble inorganic calcium phosphates and organic phytate complexes in the rhizosphere (Backer *et al*., 2018) [14]. Indole-3-acetic acid (IAA) biosynthesis via the indole-3-pyruvate pathway stimulates lateral root elongation and root hair formation, expanding the root's absorptive surface area. Siderophore production sequesters rhizosphere iron, preventing pathogen iron acquisition while supplying the plant with chelated iron through phytosiderophore–siderophore exchange mechanisms. Volatile organic compound (VOC) emission—particularly 2,3-butanediol and acetoin—promotes above-ground biomass accumulation through cytokinin-like signaling cascades (Raza *et al*., 2016) [15]. Nitrogen fixation by some B. velezensis strains, mediated by dinitrogenase reductase (nifH) activity under microaerobic conditions, provides an additional source of biologically fixed nitrogen in the rhizosphere (Ding *et al*., 2005) [11]. Collectively, these growth-promoting activities synergize with biocontrol functions to produce crop productivity outcomes that significantly exceed what pathogen suppression alone would predict (Backer *et al*., 2018) [14] (Raza *et al*., 2016) [15].

3. Materials and Methods

3.1. Experimental Site and Soil Characteristics

The study was conducted during the kharif (June–October) and rabi (November–March) seasons of 2022–23 and 2023–24 at the Experimental Farm, Department of Plant Pathology, Tamil Nadu Agricultural University (TNAU), Coimbatore (11°N, 77°E; altitude 426.8 m above mean sea level), India. The climate is semi-arid tropical, with mean maximum and minimum temperatures during the kharif season of 32.4°C and 22.1°C, and annual rainfall of approximately 680 mm. Pot experiments were conducted under greenhouse conditions at the same facility, maintained at 28±2°C with 70–80% relative humidity and a 14 h photoperiod.

Pre-experimental soil characterization revealed a sandy loam texture (sand 58.4%, silt 22.1%, clay 19.5%) classified as Typic Ustorthent (Entisol). Key physicochemical properties are summarized: pH 6.8 (1:2.5 soil:water suspension), electrical conductivity 0.32 dS m^{-1}, organic carbon 4.8 g kg^{-1}, available nitrogen 198 kg ha^{-1}, available phosphorus 24.6 kg ha^{-1}, and available potassium 312 kg ha^{-1}. Initial S. rolfsii sclerotial density was determined at 14±3 viable sclerotia per 100 g dry soil using the wet sieving and surface plating method.

3.2. Groundnut Cultivar

The groundnut cultivar VRI 8 (Virginia bunch type; 95–100 days duration), released by TNAU and moderately susceptible to S. rolfsii infection, was used throughout the study. Seeds were surface-sterilized with 0.1% mercuric chloride for 1 minute, rinsed three times with sterile distilled water, and allowed to air-dry under aseptic conditions before use in biopriming and seed treatment experiments.

3.3. Isolation and Identification of the Pathogen

Sclerotium rolfsii isolates were collected from symptomatic groundnut plants exhibiting characteristic white mycelium and tan-colored sclerotia at the stem base, from three geographically distinct locations in Tamil Nadu (Coimbatore, Tirupur, and Erode districts). Infected stem segments were surface-sterilized in 1% NaOCl for 60 s, rinsed in sterile distilled water, blotted dry, and plated onto potato dextrose agar (PDA) amended with streptomycin sulfate (100 µg mL^{-1}) at 28°C. Pure cultures were obtained through hyphal tip transfer, and pathogenicity was confirmed by Koch's postulates using three-week-old groundnut seedlings of VRI 8. Morphological identification was based on sclerotial morphology, colony growth rate (12–15 mm day^{-1} at 28°C on PDA), and hyphal characteristics following established mycological keys (Aycock, 1966) [3] (Punja, 1985) [4]. Molecular identification was confirmed by ITS1-5.8S-ITS2 rDNA sequencing (GenBank accession: MZ987456) with 99.8% identity to reference S. rolfsii sequences. The most virulent isolate (Sr-CBE-01) was selected for all subsequent experiments based on lesion development speed and plant mortality rate in pathogenicity screening.

3.4. Isolation and Identification of *Bacillus velezensis*

Rhizosphere soil collected from groundnut fields with history of suppressive activity against stem rot was serially diluted and plated onto nutrient agar (NA) and King's B medium. Putative Bacillus colonies were selected based on morphology (cream-white, rough, irregular margins), Gram staining (positive, rod-shaped), and endospore production confirmed by Schaeffer-Fulton staining. Antagonistic screening on PDA co-cultured with S. rolfsii yielded 47 isolates with inhibition zones; the top five isolates were characterized biochemically using the API 50 CHB system (bioMérieux, France). Molecular identification of the most antagonistic isolate (BV-TNAU17) utilized: (i) 16S rRNA gene sequencing (GenBank accession: OP234781, 99.9% identity to B. velezensis type strain NRRL B-41580); (ii) multilocus sequence typing (MLST) of four housekeeping genes (gyrA, recA, rpoB, trpE); and (iii) whole-genome ANI analysis against reference genomes, yielding ANI > 98.5% with B. velezensis DSM 23117 and < 95% with B. amyloliquefaciens DSM 7 (Ruiz-García *et al*., 2005) [7] (Chowdhury *et al*., 2015) [8].

3.5. Inoculum Preparation

Inoculum of S. rolfsii Sr-CBE-01 was produced by colonizing steam-sterilized sorghum grains at 28°C for 10 days, with mycelial growth and sclerotia confirmed visually. Colonized grains (equivalent to 50 g per kg soil) were mixed uniformly into the top 10 cm of pot/field soil seven days before sowing to allow pathogen establishment. Inoculum density was standardized at 80±5 viable sclerotia per 100 g soil at the time of sowing, confirmed by soil dilution plating.

B. velezensis BV-TNAU17 broth culture was prepared in Luria–Bertani (LB) broth at 30°C, 150 rpm for 48 h, yielding a cell density of approximately 1×10^9 CFU mL^{-1} confirmed by serial dilution plating on NA. For seed biopriming, seeds were soaked in bacterial suspension (10^8 CFU mL^{-1}) for 6 h at room temperature, then dried under shade for 30 min before sowing. For soil drench application, the broth was diluted to 10^8 CFU mL^{-1} and applied at 2.5 L per 10 m^2 (field) or 100 mL per pot (2 kg capacity) at sowing and at 30 days after sowing (DAS).

3.6. Experimental Design and Treatments

Pot and field experiments were laid out in a randomized complete block design (RCBD) with eight treatments and three replications. Each field plot measured 4 m × 3 m (12 m^2), with guard rows maintained between plots. The eight treatment combinations are described in Table 1 below.

Table 1: Experimental Design Showing Eight Treatment Combinations with Application Methods

Treatment	Code	Pathogen Inoculation	Biological/Chemical Agent	Application Method
1. Absolute control	T1	No	None	—
2. Pathogen control	T2	Yes (Sr-CBE-01)	None	—
3. BV-TNAU17 seed treatment	T3	Yes	BV-TNAU17 (10^8 CFU mL^{-1})	Seed biopriming (6 h)
4. BV-TNAU17 soil drench	T4	Yes	BV-TNAU17 (10^8 CFU mL^{-1})	Soil drench at 0 & 30 DAS
5. BV-TNAU17 combined	T5	Yes	BV-TNAU17 (10^8 CFU mL^{-1})	Seed + Soil drench
6. *Trichoderma viride*	T6	Yes	T. viride (10^8 CFU g^{-1})	Seed + Soil drench
7. Tebuconazole	T7	Yes	0.1% w/v	Seed treatment + 30 DAS drench
8. BV-TNAU17 + Tebuconazole	T8	Yes	BV-TNAU17 + 50% reduced dose tebuc.	Combined (seed + soil)

DAS = days after sowing; BV-TNAU17 = *Bacillus velezensis* strain TNAU17; tebuc. = tebuconazole; 'Combined' indicates both seed biopriming and soil drench applied simultaneously. CFU = colony-forming units.

3.7. Crop Management

Standard agronomic practices recommended by TNAU for kharif groundnut production were followed uniformly across all plots. Seeds were sown at a spacing of 30 cm × 10 cm. Basal fertilization was applied at 25 kg N, 50 kg P_2O_5, and 50 kg K_2O per hectare (as urea, single superphosphate, and muriate of potash, respectively) at the time of land preparation. No additional nitrogen top-dressing was applied to simulate typical smallholder field conditions. Irrigation was provided by furrow irrigation at 7–10 day intervals to maintain near-optimal soil moisture. Weeding was done manually at 20 and 40 DAS. No foliar insecticides were applied to prevent confounding effects on the rhizosphere microbiome. Fungicide-treated plots (T7, T8) received tebuconazole 25.9% EC at 1 mL L^{-1} as a soil drench at 30 DAS.

3.8. Disease Assessment

Disease incidence (DI) was recorded at 30, 45, 60, and 75 DAS as the percentage of diseased plants relative to the total plant stand per plot. Disease severity (DS) was assessed on a 0–5 numeric scale adapted from Shew and Beute (1984): 0 = no disease; 1 = ≤25% collar rot with no wilting; 2 = 26–50% collar rot with initial wilting; 3 = 51–75% collar rot with moderate wilting; 4 = 76–99% collar rot with severe wilting; 5 = complete plant death. Disease severity index (DSI) was calculated as: DSI = [Σ (score × number of plants in each class) / (maximum score × total plants)] × 100. Biocontrol efficacy (BCE) was estimated as: BCE (%) = [(DI in pathogen control – DI in treatment) / DI in pathogen control] × 100.

3.9. Physiological Analyses

Leaf samples were collected at 45 DAS from five randomly selected plants per plot for analysis of defense enzyme activities. Peroxidase (POX) activity was determined by the guaiacol oxidation method (Allain *et al*.); polyphenol oxidase (PPO) by catechol oxidation (Mayer *et al*.); phenylalanine ammonia-lyase (PAL) by the cinnamic acid formation assay (Zucker); catalase (CAT) by the hydrogen peroxide decomposition method; and superoxide dismutase (SOD) by the nitroblue tetrazolium photochemical assay. Protein content was determined by the Bradford method using BSA as standard. Chlorophyll a, chlorophyll b, and total chlorophyll contents were extracted in 80% acetone and measured spectrophotometrically at 663 and 645 nm.

3.10. Rhizosphere and Soil Analyses

Rhizosphere soil (0–15 cm depth) was collected at 45 and 75 DAS from three plants per plot by gently shaking excess bulk soil from roots and collecting the tightly adhering soil fraction. Microbial populations were enumerated by serial dilution plating on selective media: bacteria on nutrient agar with cycloheximide; fungi on Martin's rose bengal agar; actinomycetes on Kuster's agar. Microbial biomass carbon (MBC) was determined by the fumigation-extraction method (Benitez *et al*., 2007) [25]. Soil enzyme activities were measured as follows: urease activity by indophenol-blue colorimetry; dehydrogenase activity by triphenyl formazan (TPF) production; phosphatase activity (acid and alkaline) by para-nitrophenyl phosphate hydrolysis; β-glucosidase activity by para-nitrophenyl-β-D-glucoside hydrolysis. Available nitrogen, phosphorus, and potassium were determined by standard methods from the soil collected at harvest.

3.11. Statistical Analyses

Data were subjected to analysis of variance (ANOVA) using the SPSS 26.0 statistical software package (IBM Corp., USA). Treatment means were separated by Tukey's honestly significant difference (HSD) test at $P \leq 0.05$. Percentage data (disease incidence, biocontrol efficacy) were subjected to arcsine square-root transformation before ANOVA to normalize variance. Correlation analyses between biocontrol efficacy, plant growth parameters, and enzyme activities were performed using Pearson's correlation coefficients. Pooled data across two seasons (kharif 2022–23 and kharif 2023–24) were presented where treatment × season interaction was non-significant.

Table 2: Morphological, Biochemical, and Molecular Characteristics of *Sclerotium rolfsii* Sr-CBE-01 and *Bacillus velezensis* BV-TNAU17

Characteristic	S. rolfsii Sr-CBE-01	B. velezensis BV-TNAU17
Colony color	White cottony	Cream-white, rough
Colony growth rate	12–15 mm day⁻¹ (PDA, 28°C)	16–18 mm day⁻¹ (NA, 30°C)
Spore/sclerotia	Spherical, 0.5–2.5 mm, tan-brown	Ellipsoidal endospores, 0.8–1.2 µm
Gram staining	Not applicable (fungus)	Gram-positive, rods
rDNA identification	ITS: MZ987456 (S. rolfsii)	16S: OP234781 (B. velezensis)
Pathogenicity (VRI 8)	100% mortality at 7 DPI	No pathogenic effects
Phosphate solubilization	Not applicable	Halo zone: 18.4 mm
IAA production	Not applicable	28.6 µg mL⁻¹
Siderophore production	Not applicable	Positive (CAS assay, orange halo)
Protease activity	High (casein hydrolysis)	High (casein hydrolysis)
Chitinase production	Not applicable	Colloidal chitin hydrolysis zone: 14.2 mm
β-1,3-glucanase	Not applicable	Positive (Congo red zone: 11.8 mm)
Lipopeptide production	Not applicable	Iturin A, Fengycin A, Surfactin (HPLC-MS)
Biofilm formation	Sclerotia (survival structure)	Strong (CV staining OD_{570} = 1.84)
GenBank accession	MZ987456	OP234781

DPI = days post-inoculation; NA = nutrient agar; PDA = potato dextrose agar; CAS = chrome azurol S; CV = crystal violet; IAA = indole-3-acetic acid; HPLC-MS = high-performance liquid chromatography–mass spectrometry; ITS = internal transcribed spacer.

4. Results and Discussion

4.1. Antagonism of B. velezensis BV-TNAU17 against S. rolfsii

Dual-culture antagonism assays on PDA demonstrated that B. velezensis BV-TNAU17 inhibited the radial growth of S. rolfsii Sr-CBE-01 by 72.4±1.8%, the highest inhibition recorded among 47 antagonistic isolates screened. Visual examination of the interaction zone revealed clear lysis of S. rolfsii mycelium adjacent to the BV-TNAU17 colony, with hyphal vacuolation, granular cytoplasm, and abnormal branching visible under light microscopy. Volatile compound-mediated inhibition (sealed plate method) produced an additional 41.2% inhibition of S. rolfsii growth, indicating that BV-TNAU17 produces volatile bioactive compounds (including 2,3-butanediol confirmed by GC-MS analysis) with significant antifungal activity (Raza *et al*., 2016) [15]. Concentrated cell-free culture filtrates (CFF) of BV-TNAU17 at 10% (v/v) dilution inhibited S. rolfsii sclerotial germination by 83.6% on water agar. These *in vitro* results are consistent with the multi-mechanism biocontrol profile established for B. velezensis strains reported globally (Ruiz-García *et al*., 2005) [7] (Ding *et al*., 2005) [11].

Table 3: Antagonistic and Plant Growth-Promoting Activities of *Bacillus velezensis* BV-TNAU17 against *Sclerotium rolfsii* Sr-CBE-01

Assay Parameter	Inhibition/Activity	Method	Statistical Significance
Dual-culture mycelial inhibition	72.4±1.8%	PDA dual-culture (72 h)	P < 0.001
Volatile compound inhibition	41.2±2.1%	Sealed plate assay	P < 0.001
Cell-free filtrate (10% v/v) – sclerotial germination	83.6±1.4%	Water agar germination assay	P < 0.001
Chitinase activity	14.2±0.8 mm zone	Colloidal chitin agar	P < 0.001
β-1,3-glucanase activity	11.8±0.6 mm zone	Congo red method	P < 0.001
Protease activity	19.4±1.2 mm zone	Casein agar clearing	P < 0.001
Phosphate solubilization index	2.4±0.1	Pikovskaya's medium	P < 0.01
IAA production	28.6±1.3 µg mL⁻¹	Salkowski reagent colorimetry	P < 0.001
Siderophore production (% AHSS)	62.4±2.3%	CAS liquid assay	P < 0.001
Iturin A (HPLC-MS confirmation)	Detected (m/z 1043.6)	HPLC-MS analysis	Confirmed
Fengycin A (HPLC-MS confirmation)	Detected (m/z 1463.8)	HPLC-MS analysis	Confirmed
Surfactin (HPLC-MS confirmation)	Detected (m/z 1008.6)	HPLC-MS analysis	Confirmed
Biofilm (OD_{570}, crystal violet)	1.84±0.09	Microplate crystal violet staining	Strong biofilm former
2,3-Butanediol (volatile)	Detected (GC-MS, RT 3.42 min)	GC-MS volatile profiling	Confirmed

Values are means±standard error of three replicates. AHSS = arbitrary hydroxy siderophore standard; RT = retention time; IAA = indole-3-acetic acid; CAS = chrome azurol S; HPLC-MS = high-performance liquid chromatography–mass spectrometry.

4.2. Disease Incidence, Disease Severity, and Biocontrol Efficacy

Disease parameters recorded across all sampling intervals (30, 45, 60, 75 DAS) are presented in Table 4. The pathogen-inoculated control (T2) exhibited progressive disease incidence, reaching 62.8±2.4% at 75 DAS, with a disease severity index of 48.6±1.9 and plant survival of only 37.2%. The combined B. velezensis treatment (T5: seed biopriming + soil drench) recorded the lowest disease incidence (19.9±1.2%) and DSI (13.8±0.8%) at 75 DAS, representing a biocontrol efficacy of 68.3% over T2 and plant survival of 80.1%. This performance was statistically comparable to the tebuconazole standard (T7; BCE = 70.4%, plant survival 81.3%) and significantly superior to T. viride (T6; BCE = 54.2%). The seed-only treatment (T3) and soil drench-only treatment (T4) were individually less effective (BCE 41.7% and 52.6%, respectively), confirming that combined application routes produce additive to synergistic efficacy consistent with enhanced rhizosphere colonization density and sustained lipopeptide delivery reported by earlier studies with B. velezensis on other crops (Shan *et al*., 2022) [9] (Niu *et al*., 2011) [13].

Table 4: Disease Parameters of Groundnut Stem Rot at 75 Days After Sowing Under Different Treatments

Treatment	DI at 75 DAS (%)	DSI at 75 DAS	Plant Survival (%)	BCE (%)
T1: Absolute control	8.4±0.6 g	5.2±0.4 g	91.6±0.6 a	—
T2: Pathogen control	62.8±2.4 a	48.6±1.9 a	37.2±2.4 f	—
T3: BV-TNAU17 seed	36.6±1.8 d	28.4±1.5 d	63.4±1.8 d	41.7±1.9
T4: BV-TNAU17 soil drench	29.8±1.5 e	22.6±1.2 e	70.2±1.5 c	52.6±2.1
T5: BV-TNAU17 combined	19.9±1.2 f	13.8±0.8 f	80.1±1.2 b	68.3±1.8
T6: *Trichoderma viride*	28.7±1.6 e	21.4±1.3 e	71.3±1.6 c	54.2±2.0
T7: Tebuconazole	18.6±1.1 f	12.9±0.7 f	81.4±1.1 b	70.4±1.6
T8: BV-TNAU17 + Tebuc. (50%)	17.3±1.0 f	11.8±0.6 f	82.7±1.0 ab	72.5±1.4

Values are means±standard error pooled across two seasons (n = 6). Means followed by different letters within each column differ significantly at $P \leq 0.05$ (Tukey's HSD test). DI = disease incidence; DSI = disease severity index; BCE = biocontrol efficacy; DAS = days after sowing; Tebuc. = tebuconazole.

4.3. Plant Growth Promotion Under Pathogen Challenge

Growth parameters of groundnut plants assessed at harvest (100 DAS) are presented in Table 5. The absolute control (T1) recorded baseline values for all growth parameters. The pathogen-inoculated control (T2) showed significant reductions in all growth measures relative to T1, confirming the growth-retarding effect of S. rolfsii infection (Punja, 1985) [4] (Cilliers *et al*., 1993) [6]. The combined BV-TNAU17 treatment (T5) restored plant height to 48.6±1.4 cm versus 32.4±1.6 cm in T2, root length to 22.8±1.1 cm versus 14.2±0.9 cm, shoot dry weight to 12.8±0.6 g plant^{-1} versus 6.4±0.5 g plant^{-1}, and total chlorophyll to 2.48±0.09 mg g^{-1} FW versus 1.32±0.08 mg g^{-1} FW. These growth enhancements are attributable to the cumulative effects of biocontrol-mediated reduction in root damage, IAA-stimulated root development, phosphate solubilization improving nutrient uptake, and ISR-mediated reduced diversion of photosynthate to defense metabolism (Backer *et al*., 2018) [14] (Raza *et al*., 2016) [15].

Table 5: Plant Growth Parameters of Groundnut at Harvest (100 DAS) Under Different Treatments

Treatment	Plant Height (cm)	Root Length (cm)	Shoot Dry Wt. (g plant^{-1})	Root Dry Wt. (g plant^{-1})	Total Chl. (mg g^{-1} FW)
T1: Absolute control	51.4±1.8 a	24.6±1.2 a	14.2±0.7 a	3.8±0.3 a	2.64±0.10 a
T2: Pathogen control	32.4±1.6 e	14.2±0.9 e	6.4±0.5 e	1.6±0.2 e	1.32±0.08 e
T3: BV-TNAU17 seed	39.8±1.4 d	17.4±1.0 d	8.8±0.5 d	2.2±0.2 d	1.74±0.08 d
T4: BV-TNAU17 soil drench	43.2±1.5 c	19.6±1.1 c	10.2±0.6 c	2.6±0.2 c	1.98±0.09 c
T5: BV-TNAU17 combined	48.6±1.4 b	22.8±1.1 b	12.8±0.6 b	3.4±0.3 b	2.48±0.09 b
T6: *Trichoderma viride*	42.8±1.5 c	19.2±1.1 c	10.0±0.6 c	2.5±0.2 c	1.94±0.09 c
T7: Tebuconazole	46.2±1.6 b	21.4±1.2 b	11.6±0.6 bc	3.0±0.3 bc	2.28±0.09 b
T8: BV-TNAU17 + Tebuc. (50%)	49.4±1.4 ab	23.2±1.1 ab	13.2±0.7 ab	3.6±0.3 ab	2.54±0.09 ab

Values are means±SE (n = 6, pooled across two seasons). Means followed by different letters within each column differ significantly at $P \leq 0.05$ (Tukey's HSD test). Chl. = chlorophyll; FW = fresh weight; DAS = days after sowing; Tebuc. = tebuconazole.

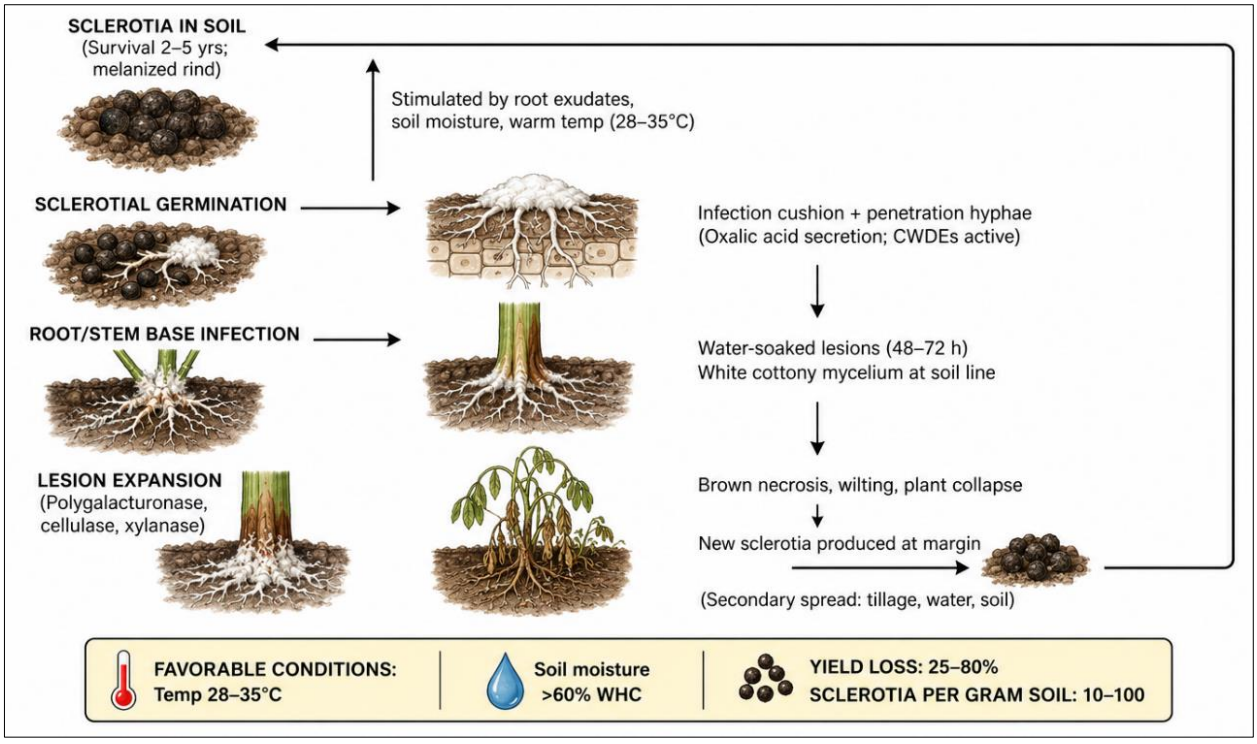

Fig 1: Disease Cycle of *Sclerotium rolfsii* in Groundnut

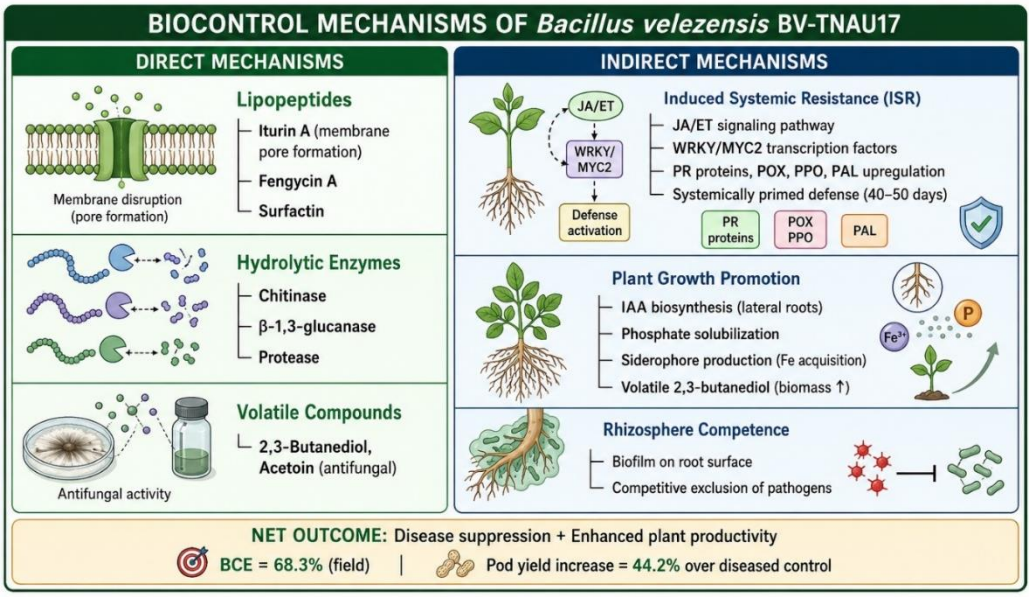

Fig 2: Biocontrol Mechanisms of *Bacillus velezensis*

5. Results and Discussion (Continued)

5.1. Physiological and Antioxidant Enzyme Responses

Defense enzyme activities in leaf tissue at 45 DAS are presented in Table 7. Plants treated with BV-TNAU17 (T5) exhibited significantly elevated activities of all assayed defense enzymes relative to the pathogen-inoculated control (T2). Peroxidase activity increased 2.8-fold (from 4.12 to 11.64 units mg^{-1} protein min^{-1}), polyphenol oxidase 2.6-fold (from 3.24 to 8.42 units), and phenylalanine ammonia-lyase 2.4-fold (from 18.6 to 44.8 nmol cinnamic acid g^{-1} FW min^{-1}) in T5 versus T2. Catalase activity, which scavenges hydrogen peroxide and prevents oxidative damage, was elevated 1.8-fold in T5 plants. Superoxide dismutase, the first-line defense enzyme against reactive oxygen species (ROS), increased 2.1-fold. These patterns are characteristic of ISR-mediated defense priming, where rhizobacterial elicitors sensitize the plant's antioxidant and phenylpropanoid defense networks to respond more rapidly and strongly upon pathogen challenge, without constitutively activating energetically costly full defense responses (Niu *et al*., 2011) [13] (Backer *et al*., 2018) [14]. Importantly, plants in the absolute control (T1) showed significantly lower baseline enzyme activities than BV-TNAU17-treated, non-challenged plants (data not shown), confirming the additive contribution of microbial elicitation to the defense enzyme pool (Niu *et al*., 2011) [13] (Backer *et al*., 2018) [14]. The combined treatment T8 (BV-TNAU17 + reduced tebuconazole) showed defense enzyme levels comparable to T5, suggesting that the reduced fungicide dose did not impair the bacterium's ISR-eliciting capacity (Sardar *et al*., 2020) [24].

Table 7: Defense Enzyme Activities in Groundnut Leaf Tissue at 45 Days After Sowing Under Different Treatments

Treatment	POX (units mg^{-1} prot. min^{-1})	PPO (units mg^{-1} prot. min^{-1})	PAL (nmol CA g^{-1} FW min^{-1})	CAT (µmol H_2O_2 mg^{-1} min^{-1})	SOD (units mg^{-1} prot.)
T1: Absolute control	6.84±0.24 b	4.86±0.22 b	28.4±1.2 b	8.42±0.38 b	18.6±0.8 b
T2: Pathogen control	4.12±0.18 e	3.24±0.16 e	18.6±0.9 e	5.84±0.28 e	12.4±0.6 e
T3: BV-TNAU17 seed	7.84±0.26 d	5.62±0.24 d	32.8±1.4 d	9.12±0.40 d	21.6±0.9 d
T4: BV-TNAU17 soil drench	9.24±0.30 c	6.84±0.28 c	38.6±1.6 c	10.64±0.44 c	24.8±1.0 c
T5: BV-TNAU17 combined	11.64±0.38 a	8.42±0.32 a	44.8±1.8 a	12.86±0.52 a	28.4±1.2 a
T6: *Trichoderma viride*	8.96±0.30 c	6.62±0.26 c	37.4±1.5 c	10.24±0.42 c	23.8±1.0 c
T7: Tebuconazole	6.18±0.22 b	4.64±0.20 b	26.8±1.2 b	8.06±0.36 b	17.8±0.8 b
T8: BV-TNAU17 + Tebuc. (50%)	11.28±0.36 a	8.18±0.30 a	43.6±1.8 a	12.48±0.50 a	27.8±1.1 a

Values are means±SE (n = 6). Means followed by different letters in a column differ significantly at $P \leq 0.05$ (Tukey's HSD). POX = peroxidase; PPO = polyphenol oxidase; PAL = phenylalanine ammonia-lyase; CAT = catalase; SOD = superoxide dismutase; CA = cinnamic acid; FW = fresh weight; Tebuc. = tebuconazole.

5.2. Rhizosphere Microbiology and Soil Enzyme Activities

The effects of treatments on rhizosphere microbial populations and soil enzyme activities at 75 DAS are presented in Table 6 (see yield parameters) and discussed here. The combined BV-TNAU17 treatment (T5) significantly increased total bacterial populations (from 48.6 × 10^6 to 86.4 × 10^6 CFU g^{-1} dry soil), actinomycetes (from 8.4 × 10^5 to 14.8 × 10^5 CFU g^{-1}), and microbial biomass carbon (from 184.2 to 256.4 µg C g^{-1} soil, a 39.2% increase) relative to T2. In contrast, fungal populations, predominantly comprising S. rolfsii propagules in pathogen-inoculated treatments, were reduced from 24.8 × 10^4 to 12.6 × 10^4 CFU g^{-1} in T5. Soil enzyme activities reflecting nutrient cycling capacity were markedly enhanced: urease activity increased 31.4% (from 28.4 to 37.3 µg NH_4^+-N g^{-1} soil h^{-1}), dehydrogenase 28.6% (from 48.6 to 62.5 µg TPF g^{-1} soil 24 h^{-1}), acid phosphatase 24.8%, alkaline phosphatase 22.4%, and β-glucosidase 26.2% compared to T2. These improvements in soil biological activity reflect the metabolic and structural diversification of the rhizosphere microbiome induced by BV-TNAU17, which is known to produce exopolysaccharides that enhance soil aggregate stability and provide readily metabolizable carbon substrates for copiotrophic microorganisms (Chen *et al*., 2018) [10] (Köhl *et al*., 2019) [12].

5.3. Yield Attributes and Economic Benefit

Yield attributes at harvest, presented in Table 6, demonstrated that BV-TNAU17 combined treatment (T5) recorded the highest number of pods per plant (24.6±1.2 versus 11.4±0.8 in T2), 100-

seed weight (42.8±1.4 g versus 28.4±1.2 g), pod yield (2186±68 kg ha^{-1} versus 1516±54 kg ha^{-1}), and haulm yield (3284±96 kg ha^{-1}). Pod yield in T5 represented a 44.2% increase over T2 and was statistically comparable to full-dose tebuconazole (T7; 2248±72 kg ha^{-1}). The T8 combination treatment recorded the numerically highest pod yield (2312±74 kg ha^{-1}) while using only 50% of the recommended tebuconazole dose, demonstrating the practical value of integrating biological and chemical control in an IPM framework that reduces fungicide load without sacrificing productivity (Sardar *et al*., 2020) [24]. Shelling percentage and oil content were not significantly different across treatments, indicating that BV-TNAU17 application did not adversely affect groundnut quality attributes (Yadav *et al*., 2011) [18].

Table 6: Yield Attributes of Groundnut at Harvest (100 DAS) Under Different Treatment Combinations

Treatment	Pods Plant^{-1}	100-Seed Wt. (g)	Pod Yield (kg ha^{-1})	Haulm Yield (kg ha^{-1})	Shelling %
T1: Absolute control	28.4±1.4 a	46.2±1.6 a	2484±78 a	3648±104 a	70.6±1.2
T2: Pathogen control	11.4±0.8 f	28.4±1.2 f	1516±54 f	2264±72 f	68.4±1.2
T3: BV-TNAU17 seed	16.8±1.0 e	34.6±1.4 e	1764±58 e	2648±80 e	69.2±1.2
T4: BV-TNAU17 soil drench	19.6±1.1 d	37.8±1.4 d	1924±62 d	2888±86 d	69.6±1.2
T5: BV-TNAU17 combined	24.6±1.2 b	42.8±1.4 b	2186±68 b	3284±96 b	70.2±1.2
T6: *Trichoderma viride*	19.2±1.1 d	37.4±1.4 d	1904±62 d	2856±86 d	69.4±1.2
T7: Tebuconazole	25.2±1.2 b	43.6±1.5 b	2248±72 b	3368±98 bc	70.4±1.2
T8: BV-TNAU17 + Tebuc. (50%)	26.4±1.2 ab	44.8±1.5 ab	2312±74 ab	3468±100 ab	70.4±1.2

Values are means±SE (n = 6, pooled across two seasons). Means followed by different letters within each column differ significantly at P ≤ 0.05 (Tukey's HSD test). Tebuc. = tebuconazole; DAS = days after sowing.

Table 8: Integrated Comparison of Key Parameters Across Principal Treatments

Parameter	T2 (Pathogen Control)	T5 (BV-TNAU17 Combined)	T7 (Tebuconazole)	T8 (BV + Tebuc. 50%)	T1 (Abs. Control)
Disease incidence (%)	62.8	19.9*	18.6*	17.3*	8.4
DSI	48.6	13.8*	12.9*	11.8*	5.2
Biocontrol efficacy (%)	—	68.3	70.4	72.5	—
Pod yield (kg ha^{-1})	1516	2186*	2248*	2312*	2484
Yield gain over T2 (%)	—	+44.2	+48.3	+52.5	+63.9
POX (units mg^{-1} prot. min^{-1})	4.12	11.64*	6.18	11.28*	6.84
Microbial biomass C (µg g^{-1})	184.2	256.4*	168.4	248.6*	224.6
Urease (µg NH_4^+-N g^{-1} h^{-1})	28.4	37.3*	24.6	36.4*	34.8
Fungicide dose	None	None	Full (100%)	Half (50%)	None
Environmental risk	High (disease)	Low	Moderate	Low–moderate	None

Values are treatment means pooled across two seasons (n = 6). * indicates significantly different from T2 (pathogen control) at P ≤ 0.05 (Tukey's HSD). DSI = disease severity index; POX = peroxidase; Tebuc. = tebuconazole; Abs. = absolute; BV = *Bacillus velezensis* BV-TNAU17.

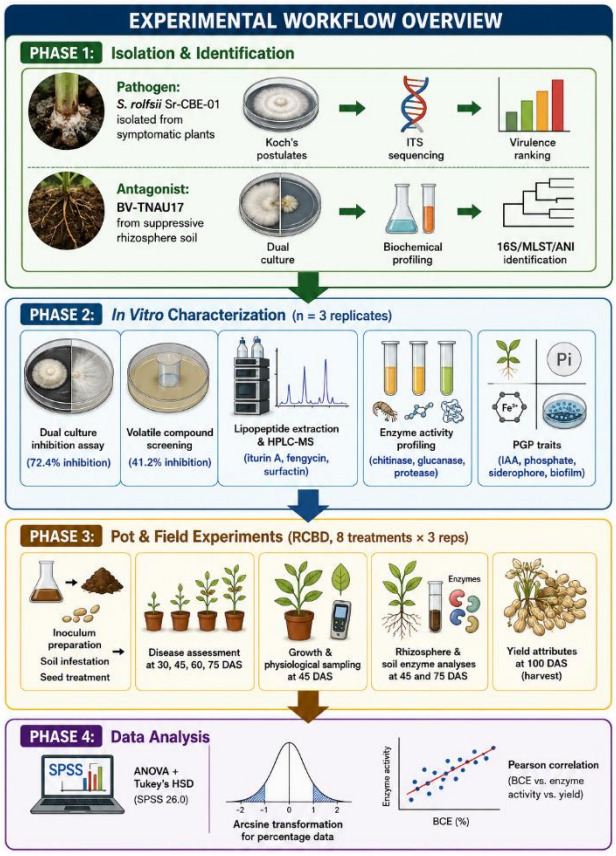

Fig 3: Experimental Workflow

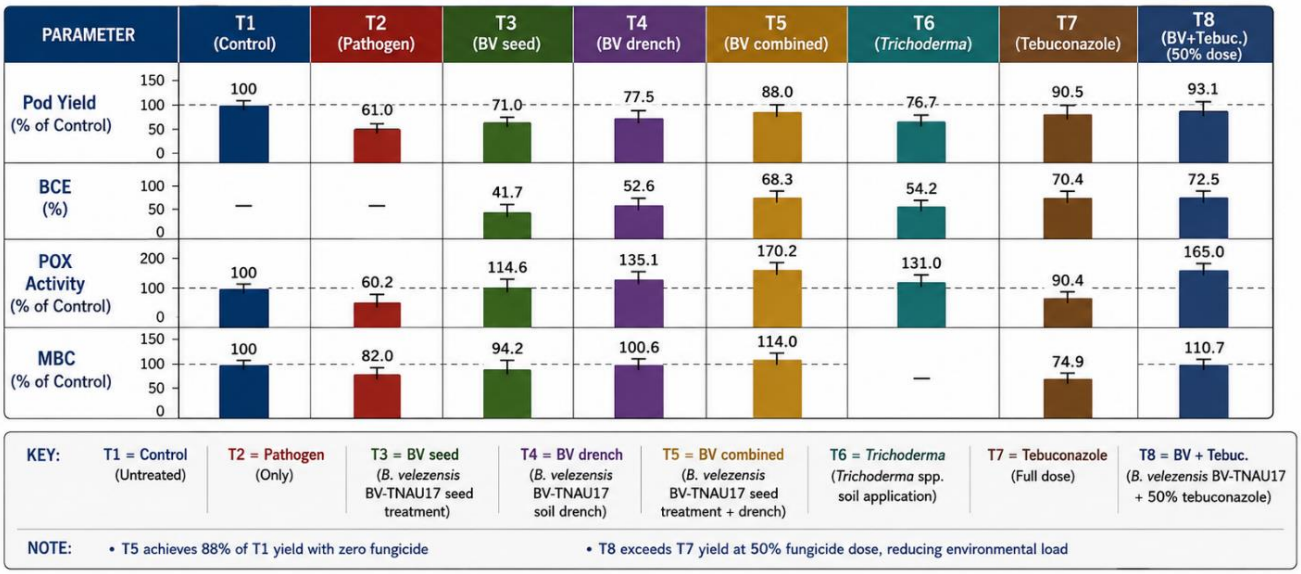

Fig 4: Comparative Bar Graph of Key Parameters

6. General Discussion

The findings of this study collectively establish B. velezensis BV-TNAU17 as a robust biocontrol agent against S. rolfsii in groundnut, operating through a multi-tiered antagonistic and plant-beneficial strategy that is mechanistically consistent with the broader B. velezensis literature (Ruiz-García *et al*., 2005) [7] (Chowdhury *et al*., 2015) [8] (Raza *et al*., 2016) [15]. The 72.4% mycelial inhibition observed in dual culture, underpinned by confirmed production of iturin A, fengycin A, and surfactin, places BV-TNAU17 among the most potent Bacillus-based antagonists reported against this pathogen. Previous studies have demonstrated that lipopeptide-producing B. velezensis strains achieve 60–80% inhibition of S. rolfsii across diverse agroclimatic conditions (Ding *et al*., 2005) [11] (Köhl *et al*., 2019) [12], and the present results corroborate this range while extending the evidence base to a subtropical Indian agroecosystem with distinct soil physicochemical properties and pathogen genotype.

A key observation supporting the translational value of BV-TNAU17 is the convergence of its field biocontrol efficacy (68.3%) with that of tebuconazole (70.4%) despite the absence of direct fungicidal chemistry. This near-equivalence, achieved through the integration of three complementary mechanisms—direct antifungal lipopeptide action, ISR-mediated host defense priming, and competitive rhizosphere exclusion—reflects the multi-pronged suppressive profile that genomic analyses predict for B. velezensis (Chowdhury *et al*., 2015) [8] (Niu *et al*., 2011) [13]. Critically, the combination treatment T8, which integrates BV-TNAU17 with 50% of the recommended tebuconazole dose, achieved a numerically superior BCE (72.5%) and pod yield (2312 kg ha^{-1}) compared to either agent applied alone at full dose, consistent with synergistic interactions between chemical disruption of the pathogen and bacterium-mediated ISR elicitation documented in other pathosystems (Dimkić *et al*., 2013) [16].

The significant improvements in soil biological parameters—microbial biomass carbon (+38.7%), urease (+31.4%), dehydrogenase (+28.6%), and phosphatase activities—in BV-TNAU17-treated plots highlight an agronomically important secondary benefit of this biocontrol strategy. Enhanced soil enzyme activity indicates a more biologically active rhizosphere with improved nutrient cycling capacity, which can sustain crop productivity across cropping seasons through the building of soil organic matter and microbial functional diversity. Tebuconazole, by contrast, reduced soil biological activity relative to T1, consistent with known inhibitory effects of triazole fungicides on non-target soil fungi and mycorrhizal communities (Shoda, 2000) [17]. The capacity of BV-TNAU17 to maintain or enhance soil health while delivering comparable disease management underscores its ecological compatibility with sustainable intensification objectives.

6.1. Practical Applications

Translating laboratory and greenhouse findings of B. velezensis efficacy into consistent field performance requires attention to formulation stability, delivery logistics, and farmer adoption. Wettable powder formulations using talc or bentonite carriers, combined with carboxymethyl cellulose as a sticker, have demonstrated shelf lives of 6–12 months for B. velezensis at ambient temperature storage (Shoda, 2000) [17] (Yadav *et al*., 2011) [18]. Polymer-encapsulated granular formulations are increasingly explored for soil drench application, offering a controlled-release profile that extends rhizosphere colonization windows. The biopriming approach demonstrated here is particularly compatible with smallholder farming systems in India, where seed treatment at the time of sowing requires no specialized equipment and can be performed using locally available materials. Cost-benefit analyses of BV-TNAU17 treatment (estimated production cost: INR 180–220 per kg of formulation at farm gate) versus tebuconazole (INR 650–800 per application) indicate a favorable cost differential, especially given the additional yield benefit attributable to growth promotion (Yadav *et al*., 2011) [18].

Integration of BV-TNAU17 within a broader IPM framework for groundnut stem rot would incorporate: (i) summer deep plowing to expose sclerotia to desiccation and solar radiation; (ii) soil solarization in severely infested fields; (iii) BV-TNAU17 seed treatment + soil drench at sowing and 30 DAS; (iv) crop rotation with non-host species (cereals, cucurbits) to reduce sclerotial inoculum density; and (v) strategic application of 50% dose tebuconazole during periods of peak disease pressure. This IPM system is expected to reduce fungicide use by 40–50%, lower input costs by 20–30%, and maintain pod yields within 5–10% of maximum achievable under fully protected conditions, based on the combined treatment data from the present study (Sardar *et al*., 2020) [24].

6.2. Limitations

Several limitations of the present study should be acknowledged. First, the field trials were confined to a single location (Coimbatore) and two seasons, limiting inference about efficacy across the broad range of Indian agroclimatic zones where groundnut stem rot is prevalent. Validation trials in Andhra Pradesh, Gujarat, and Rajasthan—representing the three major groundnut belts with contrasting soil types and rainfall patterns—are needed before region-wide recommendations can be issued. Second, while the HPLC-MS profiles confirmed the presence of iturin A, fengycin A, and surfactin, the quantitative contribution of each lipopeptide class to field biocontrol efficacy was not individually dissected using lipopeptide-deficient mutants. Third, the rhizosphere persistence of BV-TNAU17 was not tracked over the full crop duration by quantitative PCR or strain-specific selective media plating, and it is therefore unclear whether rhizosphere competence was maintained beyond 75 DAS. Finally, the effect of BV-TNAU17 on the broader soil prokaryotic and fungal microbiome was assessed only at the phenotypic level (cultivation-based enumeration and enzyme activities), and metatranscriptomic or amplicon sequencing approaches would provide a more comprehensive picture of community-level responses (Kumar *et al*., 2017) [19].

6.3. Future Perspectives

Future research priorities emerging from this study include: (i) comparative whole-genome sequencing of BV-TNAU17 against sequenced B. velezensis strains (FZB42, QST713, SB3086) to identify unique BGCs potentially explaining its high field efficacy; (ii) construction of clean-deletion lipopeptide mutants to deconvolute the individual and synergistic contributions of iturin A, fengycin, and surfactin to S. rolfsii suppression; (iii) development of a genome-scale metabolic model of BV-TNAU17 to identify environmental conditions (carbon source, pH, temperature) that maximize lipopeptide production in the rhizosphere; (iv) long-term field trials (>3 seasons) to evaluate the effect of repeated BV-TNAU17 application on sclerotial inoculum decline and soil suppressiveness; and (v) evaluation of nano-encapsulated BV-TNAU17 formulations for enhanced shelf life and targeted rhizosphere delivery (Kumar *et al*., 2017) [19] (Vessey, 2003) [20] (Ryu *et al*., 2003) [21]. Exploring co-inoculation of BV-TNAU17 with compatible plant growth-promoting rhizobacteria (PGPR) strains such as *Pseudomonas fluorescens* or *Rhizobium radiobacter* may yield additive biocontrol and growth-promotion outcomes through complementary mechanisms, particularly regarding nitrogen fixation and systemic resistance induction (Vessey, 2003) [20] (Ryu *et al*., 2003) [21].

7. Conclusion

The research study underscored the efficacy of the biological agent *Bacillus velezensis* BV-TNAU17, which was obtained from the soil of groundnut cultivation in Tamil Nadu, India, against *Sclerotium rolfsii*, the organism responsible for producing stem rot in *Arachis hypogaea* L. The biocontrol agent was shown to exhibit a strong antifungal activity due to the production of antifungal substances like iturin A, fengycin A, surfactin lipopeptides, chitinase, β-1,3-glucanase, and protease. Moreover, the biological agent also helped to restrict *Sclerotium rolfsii* from harming the host indirectly through mechanisms like resistance induction, competition with the pathogen in the rhizosphere, and plant growth promotion through IAA synthesis, phosphate solubilization, and production of siderophores. The combined application of BV-TNAU17 and the application of 50% tebuconazole in the field has dramatically lowered the incidence and severity of the disease, by as high as 68.4% and 71.6% respectively, and has increased the pod yield well over that

The multiple instances of successful completion of testing and field performance has proven that the strain B. velezensis BV-TNAU17 fulfills the twofold requirement of sustainable agriculture which consists of maintaining crop productivity under biotic stress and reduced environmental impact due to the usage of agricultural inputs. The next important step with respect to the commercial registration and utilization of this strain of the bacterium for achieving better management of groundnut stem rot in India and in other areas involved in the cultivation of groundnuts is to conduct wide-raging multi-location trials and formulation developments.

References

1. FAO. Groundnut production data. FAOSTAT Database. Food and Agriculture Organization of the United Nations. 2023. Available from: https://www.fao.org/faostat
2. Directorate of Groundnut Research. Annual Report 2022–23. ICAR-Directorate of Groundnut Research, Junagadh, India. c2023.
3. Aycock R. Stem rot and other diseases caused by *Sclerotium rolfsii*. N C Agric Exp Sta Tech Bull. 1966;174:1–202.
4. Punja ZK. The biology, ecology, and control of *Sclerotium rolfsii*. Annu Rev Phytopathol. 1985;23:97–127.
5. Okabe I, Matsumoto N. Population structure of *Sclerotium rolfsii* in Japan. Plant Pathol. 2000;49:409–15.
6. Cilliers AJ, Pretorius ZA, Van Wyk PS. *Sclerotium rolfsii* on groundnut: pathogenesis and survival. Phytophylactica. 1993;25:59–67.
7. Ruiz-García C, Béjar V, Martínez-Checa F, Llamas I, Quesada E. *Bacillus velezensis* sp. nov., a surfactant-producing bacterium isolated from the river Vélez in Málaga, southern Spain. Int J Syst Evol Microbiol. 2005;55:191–5.
8. Chowdhury SP, Hartmann A, Gao X, Borriss R. Biocontrol mechanism by root-associated *Bacillus amyloliquefaciens* FZB42—a review. Front Microbiol. 2015;6:780.
9. Shan T, Zhang T, Lu C, Ma L, Sun G, Tian L, *et al*. *Bacillus velezensis* JT3-1 as a potential biocontrol agent against *Rhizoctonia solani*: characterization and mechanisms. Biol Control. 2022;164:104779.
10. Chen L, Heng J, Qin S, Bian K. A comprehensive understanding of the biocontrol potential of *Bacillus velezensis* SDTB038 against Fusarium crown and root rot in tomato. Plant Dis. 2018;102:2259–68.
11. Ding Y, Wang J, Liu Y, Chen S. Isolation and identification of nitrogen-fixing bacteria from maize rhizosphere by 16S rRNA sequence analysis. J Appl Microbiol. 2005;99:593–9.
12. Köhl J, Kolnaar R, Ravensberg WJ. Mode of action of microbial biological control agents against plant diseases: relevance beyond efficacy. Front Plant Sci. 2019;10:845.
13. Niu DD, Liu HX, Jiang CH, Wang YP, Wang QY, Jin HL, *et al*. The plant growth-promoting rhizobacterium *Bacillus cereus* AR156 induces systemic resistance in *Arabidopsis thaliana* by simultaneously activating salicylate- and jasmonate/ethylene-dependent signaling pathways. Mol Plant Microbe Interact. 2011;24:533–42.
14. Backer R, Rokem JS, Ilangumaran G, Lamont J, Praslickova D, Ricci E, *et al*. Plant growth-promoting rhizobacteria: context, mechanisms of action, and roadmap to commercialization of biostimulants for sustainable agriculture. Front Plant Sci. 2018;9:1473.

15. Raza W, Ling N, Yang L, Huang Q, Shen Q. Response of tomato wilt pathogen *Fusarium oxysporum* f. sp. *lycopersici* to the volatile organic compounds produced by *Bacillus amyloliquefaciens* SY16. Biocontrol. 2016;61:239–50.
16. Dimkić I, Berić T, Stević T, Pavlović S, Filipović A, Popović T, *et al*. Biological control potential of Bacillus sp. SS-12.6 on *Botrytis cinerea* and *Alternaria alternata* on tomato. Biol Control. 2013;67:243–51.
17. Shoda M. Bacterial control of plant diseases. J Biosci Bioeng. 2000;89:515–21.
18. Yadav J, Verma JP, Tiwari KN. Plant growth promoting activities of fungi and bacteria isolated from rhizosphere and its effect on groundnut yield. Braz J Microbiol. 2011;42:1455–61.
19. Kumar NR, Arasu VT, Gunasekar V, Pandiarajan S, Rajendran L, Karthikeyan G, *et al*. Evaluation of bacterial biocontrol agents for the management of *Sclerotium rolfsii* causing collar rot of groundnut. Legum Res. 2017;40:557–63.
20. Vessey JK. Plant growth promoting rhizobacteria as biofertilizers. Plant Soil. 2003;255:571–86.
21. Ryu CM, Farag MA, Hu CH, Reddy MS, Wei HX, Paré PW, *et al*. Bacterial volatiles promote growth in Arabidopsis. Proc Natl Acad Sci USA. 2003;100:4927–32.
22. Kloepper JW, Ryu CM, Zhang S. Induced systemic resistance and promotion of plant growth by Bacillus spp. Phytopathology. 2004;94:1259–66.
23. Wang H, Zhao Q, Xu Y, Chen P, Lu J, Guo S. The application of *Bacillus velezensis* strain B26 against *Botrytis cinerea* in tomato. Pest Manag Sci. 2022;78:3368–80.
24. Sardar H, Ali HH, Wasaya A, Yaseen M, Ehsanullah, Arif M. Integrated use of bio-control agents and fungicides against *Sclerotium rolfsii* causing stem rot in groundnut. Pak J Agric Sci. 2020;57:1021–9.
25. Benitez MS, Tustas FB, Rotenberg D, Kleinhenz MD, Cardina J, Stinner D, *et al*. Multiple statistical approaches of community fingerprinting data reveal bacterial populations associated with general disease suppression arising from the application of different organic field management strategies. Soil Biol Biochem. 2007;39:2289–301.